Artificial Intelligence in Geosciences 4 (2023) 111–118

Contents lists available at ScienceDirect

Artificial Intelligence in Geosciences

journal homepage: www.keaipublishing.com/en/journals/artificial-intelligence-in-geosciences

Determination of future land use changes using remote sensing imagery and artificial neural network algorithm: A case study of Davao City, Philippines

Cristina E. Dumdumaya [a], Jonathan Salar Cabrera [a,b,*]

[a] College of Information and Computing, University of Southeastern Philippines, Brgy. Obrero, Davao City, Philippines
[b] Faculty of Computing, Data Sciences, Engineering and Technology, Davao Oriental State University, Mati City, Davao Oriental, 8200, Philippines

A R T I C L E I N F O

Keywords:
LULC
Artificial neural network
Remote sensing
Land use land cover prediction
Multilayer perception
Philippines

A B S T R A C T

Land use and land cover (LULC) changes refer to alterations in land use or physical characteristics. These changes can be caused by human activities, such as urbanization, agriculture, and resource extraction, as well as natural phenomena, for example, erosion and climate change. LULC changes significantly impact ecosystem services, biodiversity, and human welfare. In this study, LULC changes in Davao City, Philippines, were simulated, predicted, and projected using a multilayer perception artificial neural network (MLP-ANN) model. The MLP-ANN model was employed to analyze the impact of elevation and proximity to road networks (i.e., exploratory maps) on changes in LULC from 2017 to 2021. The predicted 2021 LULC map shows a high correlation to the actual LULC map of 2021, with a kappa index of 0.91 and a 96.68% accuracy. The MLP-ANN model was applied to project LULC changes in the future (i.e., 2030 and 2050). The results suggest that in 2030, the built-up area and trees are increasing by 4.50% and 2.31%, respectively. Unfortunately, water will decrease by up to 0.34%, and crops is about to decrease by approximately 3.25%. In the year 2050, the built-up area will continue to increase to 6.89%, while water and crops will decrease by 0.53% and 3.32%, respectively. Overall, the results show that anthropogenic activities influence the land's alterations. Moreover, the study illustrates how machine learning models can generate a reliable future scenario of land usage changes.

1. Introduction

Land use and land cover (LULC) change is a critical research topic that holds significant understanding in transforming the Earth's surface. LULC change encompasses actions such as deforestation, urbanization, and agricultural expansion that alter the Earth's surface and significantly impact ecosystems and climate change. According to a study by Houghton et al. (2012), LULC change significantly contributes to global carbon and water cycle alteration. Land use refers to the utilization that land serves, for example, recreation, agriculture, wildlife sanctuary, and many more (Saputra and Lee, 2019). Land cover refers to the top layer of the earth, including built-up infrastructure, vegetation, water, bare soil, and many more. Resource management monitoring depends on the identification and delineation of the land cover. This can be achieved by correctly recognizing the LULC, which must first be established through monitoring the baseline thematic data obtained from ground cover information. Land use management must use both the baseline data map and the subsequent change map during monitoring to identify the recent extent of land type and to recognize the land use changes from time to time. With this, LULC monitoring is usually performed using surveys, computer simulations, and modeling.

Modeling and simulating LULC changes provide valuable baseline information for forecasting future development scenarios. These models can assist in land use planning by identifying land use problems such as degradation and deforestation (Ren et al., 2019; Xia et al., 2016). Land use changes have long been crucial to urban planning. As a result, a vast amount of research is focused on understanding these changes by identifying the primary key drivers that influence the changes A study by Verburg et al. (2004) proposes the need for innovative techniques to accurately measure the effects of neighboring areas, considering the complexity of the land use systems. Furthermore, this study underscores the significance of integrating temporal dynamics to achieve a higher level of integration across models examining land use changes. These models include transportation, demographic, erosion, and groundwater, all impacting land use cover.

The land use changes have significantly impacted human activity patterns, influencing the potential for current and future inhabitation (Losiri et al., 2016). Recently, several studies focused on the

* Corresponding author. College of Information and Computing, University of Southeastern Philippines, Brgy. Obrero, Davao City, Philippines.
E-mail address: jonathan.s.cabrera85@gmail.com (J.S. Cabrera).

https://doi.org/10.1016/j.aiig.2023.08.002
Received 7 February 2023; Received in revised form 7 June 2023; Accepted 18 August 2023
Available online 25 August 2023

transformation of LULC in the Asian continent. Zhu et al. (2022) used Geographic Information System (GIS) technology to track and forecast land use changes. Likewise, Kelly-Fair et al. (2022) Used this tool, in conjunction with multicriteria analysis (MCA), to integrate of various factors by assigning weights based on decision-makers or planners' inputs. As a result, this approach makes evaluating each criterion's relative effects on the LULC modeling easier. However, the subjectivity of the input for the weights is a limitation in the model (Chang et al., 2018). The Artificial Neural Network (ANN) approach may be employed to address the weakness of multicriteria analysis. In the work of Saputra and Lee (2019), an ANN model was used to simulate multiple land-use changes and complex land-use systems. It was utilized to predict LULC changes while considering the influencing factors.

In a recent study, Cabrera and Lee (2022) suggested the localization of coastal zone management implementation due to the distinctiveness of the coastal environment. Hence, this study estimates future land use changes in a highly urbanized coastal city in the southern part of the Philippines. The researchers expect to offer insightful information for the area's future developments by analyzing the current LULC patterns and applying various modeling techniques, such as GIS and remote Sensing.

2. Related literature

LULC changes are occurring rapidly in Southeast Asian (SEA) countries, generally associated with population growth, economic development, and competing demands for land (Lambin et al., 2003). The most common changes include urban expansion, loss of agricultural land, re/deforestation, logging, and many more (Vadrevu et al., 2019). This is evident in countries like Malaysia and Indonesia, where large-scale deforestation for palm oil plantation expansions has been happening continuously to address the demands of palm oil in the international market (Koh and Wilcove, 2008). On the other hand, most developing countries, aside from small-scale deforestation caused by indigenous agriculture due to poverty, also suffer from rapid urbanization (Seto et al., 2022). These drivers of LULC changes vary widely in the SEA region. Understanding the variation of LULC is achieved by continually monitoring the geographic distribution of the land use pattern. Remote Sensing (RS) with GIS application, urban pattern detection using GIS, and ANN algorithm to generate LULC, were applied to understand the land changes.

2.1. Satellite imagery classification algorithms and remote sensing application

RS measures a region's radiation and reflects from a distance to survey and monitor its physical features. Remotely sensed imagery of the Earth is gathered using specialized cameras. A GIS is designed to capture, store, manipulate, analyze, manage, and present spatial or geographic data (Chao et al., 2022). GIS can identify and investigate the configuration of urban expansion concerning the land use pattern (Handayani et al., 2018).

RS data with various spatial resolution and image analysis techniques have been applied to monitor urban expansion (Handayani et al., 2018). RS data images are multispectral and contain rich spectral information, which has always been essential data in LULC research (Ren et al., 2019). In multispectral data, the most appropriate bands and color combinations are selected to facilitate the interpretation process of information extraction (classification) (Ren et al., 2019). A band configuration of red (4), green (3), and blue (2) is used in the natural color composite. It accurately reproduces what the human eye can see. Near-infrared (5), red (4), and green (3) make up the composite color infrared band. For studying vegetation, this band combination is helpful. SWIR-1(6), SWIR-2(7), and red(4) are the components of the short-wave infrared combination. Green tones are used to depict the vegetation in this collage. The agriculture band combination uses frequencies 6, 5, and 2 for agricultural monitoring. 7, 6, and 2 are the bands best for identifying geological structures. The 4, 3, and 1 band combination is helpful for studies of aerosols, bathymetry, and the coast. Establishing a classification system suitable for the study area is the basis of remote sensing classification using GIS image classification techniques (Chang et al., 2018). There are many sources of the S dataset. Thus, it creates ambiguity and unreliability in standardizing the dataset for LULC research. The classified images need to be compared with the actual data (i.e., ground control point data) to ensure the reliability of the classification results (Ren et al., 2019). Then, the confusion matrix's kappa coefficient (K) and other accuracy tests are used to evaluate the classification accuracy.

The study of Handayani et al. (2018) applied geospatial analysis using multi-spatial resolution data to determine the urban expansion of Surabaya, Indonesia. This study used several RS images to generate LULC change. The accuracy assessment was tested to the 500 ground truth points using post-classification to produce overall accuracy (OA) and K. Likewise, in the study of Sharma et al. (2018), a GIS-based integrated modeling approach was demonstrated to analyze the spatial pattern of LULC.

Another method for LULC classification that makes use of the phenology of RS (MODIS) pictures and the pattern similarity of time series of enhanced vegetation index (EVI) variations is the k-means method (Sato et al., 2019). The MODIS has a high temporal observation frequency but limited geographic resolution. The MODIS image is suitable for vegetation dynamics analysis (Sato et al., 2019), like typhoons and other natural calamities, due to its short monitoring interval.

A study for the impact of land cover change on ecosystem services in a tropical forested landscape used Landsat images (Talukdar et al., 2020), the Landsat 7 Enhanced Thematic Mapper (ETM+), and Landsat 8 Operational Land Imager (OLI) (https://earthexplorer.usgs.gov). It used the maximum likelihood algorithm to classify the LULC type of the RS datasets. Moreover, the LULC accuracy assessment was verified using random sampling points (Sharma et al., 2018). According to Johnson et al. (2015), the residential regions might also be extracted from the Landsat imagery using unsupervised segmentation parameter optimization (USPO). A random forest method can be helpful in accurately evaluating the LULC classification of the Landsat imagery (Cengiz et al., 2023). Tran et al. (2019) study applied the object-based image classification method to the high-resolution images of drought and human impacts on LULC change in the coastal areas of Vietnam.

Several image classification techniques can be applied to LULC classification in high and multispectral imagery. The conformity of the type of satellite image and the suitable image classification technique is not presented here. Therefore, no study asserts that any technique is the most suitable and accurate for the LULC classification.

2.2. Artificial neural network (ANN) to generate LULC

The utilization of the artificial neural network (ANN) algorithm presents a robust approach to modeling complex behaviors (Pijanowski et al., 2002). Unlike the multivariate approach, the ANN algorithm does not necessitate assumptions regarding spatial autocorrelation and multi-collinearity of the data (Pijanowski et al., 2002). This makes it particularly advantageous for predicting future land use patterns. The ANN algorithm proves valuable in geospatial land use studies due to its ability to capture complex non-linear interactions and effectively handle extensive datasets. In recent years, employing ANN models for forecasting land use changes has gained popularity. By comprehensively modeling the intricate interactions between land use and environmental factors, ANN offers enhanced precision and reliability. The environmental factors influencing land use include climate change, soil degradation, deforestation, urbanization, and water resource availability. Climate pattern variations directly impact land use and subsequently influence alterations in agricultural practices (FAO, 2007; Vorosmarty et al., 2000). Soil degradation, which affects agricultural productivity

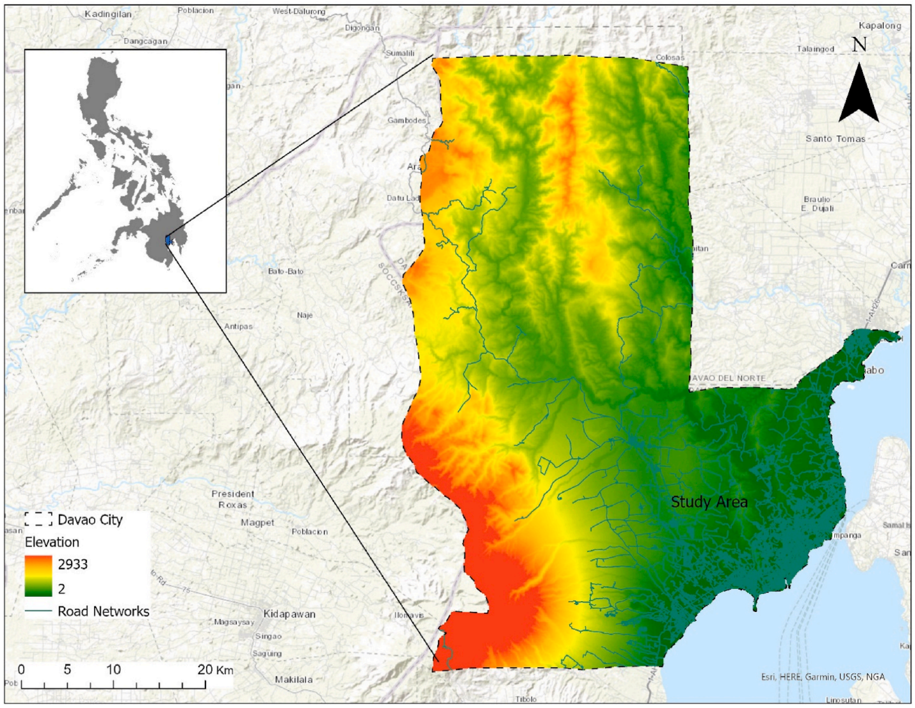

Fig. 1. Map and the elevation of Davao City and the Philippines.

Table 1
Datasets summary and the LULC maps used in this study.

Data	Criteria	Map	Year	Description	Source	Format
DEM	Elevation	Exploratory map	2017	STRM with 10 × 10 m grid resolution	United State Geological Survey (USGS)	GeoTIFF
Road map	Distance to the road network	Exploratory map	2021	Main and secondary roads of Davao City	Open Street Map	Shapefile
LULC maps	2017, 2021	Input map	2017, 2021	Sentinel-2 10 × 10 m resolution	ESRI Land Cover (https://livingatlas.arcgis.com/landcover/)	GeoTIFF

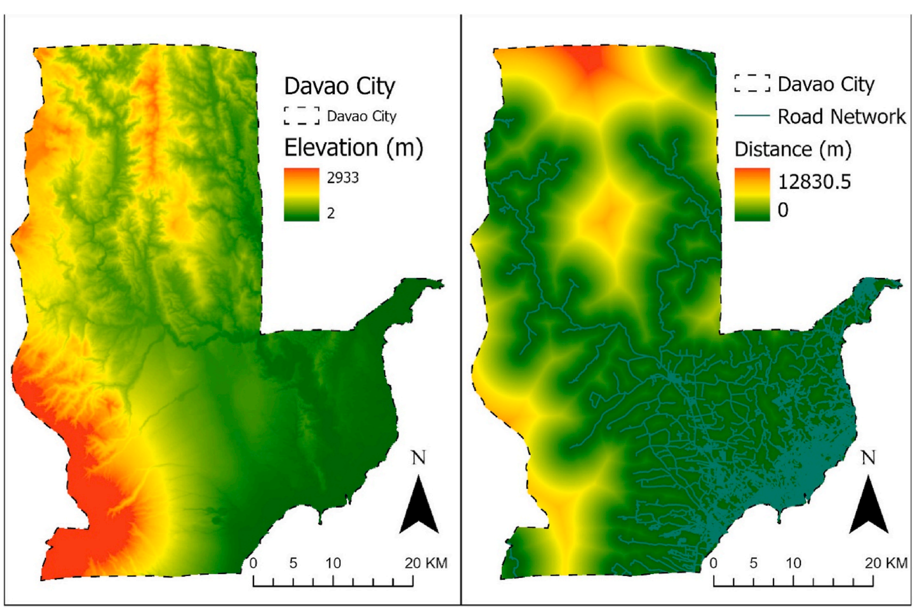

Fig. 2. Exploratory maps of the simulation. (Left) Elevation map. (Right) Road network and the distance to the road network maps.

Table 2
Eleven LULC classifications based on ESRI land cover classification.

No	Classification	Description
1	Water	Areas with permanent bodies of water; do not encompass locations with fleeting or ephemeral water presence; scarce vegetation, rocks, or human-constructed structures such as docks are absent; examples include rivers, lakes, oceans, and salt plains that are inundated.
2	Trees	Area with a high concentration of tall and dense vegetation (around 15 m or more). A closely knit canopy typically characterizes these; examples: are forests, areas with densely packed tall plants in savannas, plantations, swamps, and mangroves (locations with abundant vegetation and water that is obscured by the thickness of the canopy).
3	Flood vegetation	Areas where vegetation and water coexist throughout the year. Areas that experience periodic flooding have a combination of grass, shrubs, trees, and bare ground. Examples are mangroves inundated with water, plants growing in water, rice paddies, and other agricultural lands with heavy water management and inundation.
4	Crops	Agricultural lands with crops grown by humans, not reaching the height of trees; examples: corn, wheat, soy, structured land without crops.
5	Built Area	Man-made structures; major roadways and railway networks; large surfaces that don't absorb water, like parking lots, office buildings, and houses; examples: houses, urban areas, paved roads, asphalt.
6	Bare ground	Areas with rocks or soil and minimal to no vegetation year-round; vast regions of sand and deserts with scarce vegetation; examples: exposed rock or soil, deserts, sand dunes, dry salt flats, dried lake beds, mines.
7	Clouds	Areas where persistent cloud cover makes it impossible to determine the land cover.
8	Rangeland	Open areas covered with uniform grass with limited tall vegetation; wild cereals and grasses without human cultivation (not a farmed field); examples: natural meadows and fields with scarce tree cover, open savannas with few trees, parks, golf courses, lawns, pastures.

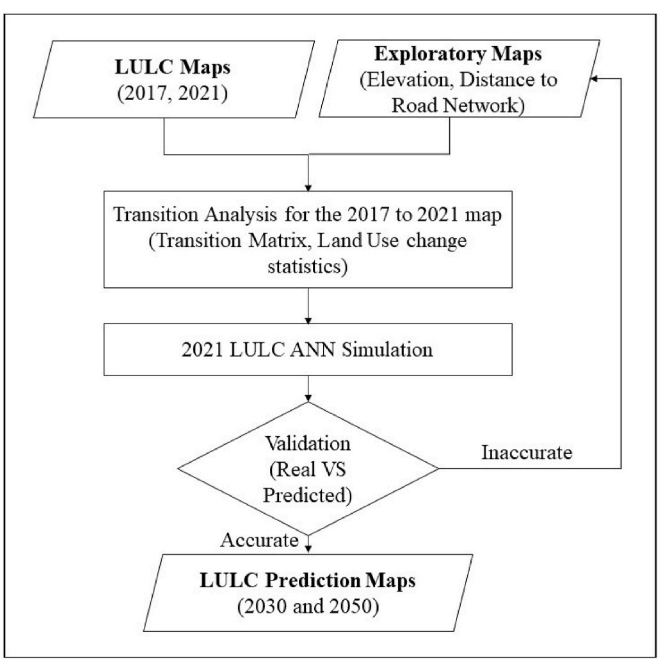

Fig. 3. The methodological framework for LULC simulation, prediction, and projection.

and restricts land suitability for certain uses, can trigger land use change (Jie et al., 2002). Deforestation for urbanization, agriculture, or logging disrupts land use patterns and ecological equilibrium (Lambin et al., 2003). The rapid expansion of urban areas contributes to losing open spaces and green landscapes (Seto et al., 2011; Xiao et al., 2022).

This study investigates the multilayer perception artificial neural network (MLP-ANN), which has gained recognition as a highly reliable neural network model. MLP-ANNs have demonstrated their effectiveness in pattern recognition and classification tasks (Amgoth et al., 2023; Dinda et al., 2022; Silva et al., 2020). The neural network model encompasses an input layer, hidden layers, and an output layer (Bocco et al., 2014; Isabona et al., 2022; Megahed et al., 2015). MLP-ANNs are widely used in LULC analysis. The MLP-ANNs' strength is the ability to deal with the complexity and non-linearity of LULC data, making them suitable for analyzing and classifying land use patterns using remotely sensed imagery. These models use spectral, and spatial information from satellite imagery, as input to the models. MLP-ANNs can learn to associate these input features with specific LULC classes through training. This enables accurate classification and analysis of LULC patterns. The MLP-ANN model was used in the study to manage and analyze large datasets and make land use change projections. The study aimed to forecast land use changes by leveraging the strengths of MLP-ANN models.

3. Study area

3.1. Study area

Davao City (as shown in Fig. 1) is a 1st class city, with an annual average income of at least 500 million pesos or roughly 9 million USD. It is also categorized as a highly urbanized city in the southern part of the Philippines. Davao City boasts the largest land area in the country, with a total land area of 2443.61 km^2 (Cabrera and Lee, 2022). Notably, it is home to Mt. Apo, the highest mountain in the Philippines. It is also the most populated city on Mindanao Island and the third most populous city in the Philippines (Cabrera and Lee, 2022). It has a population of 1, 776,949 (PSA, 2020). The city serves as Mindanao's leading trade, commerce, and industry hub.

3.2. Data, maps, and criteria

The data used in this study comprise road networks, a digital elevation model (DEM), and two LULC maps for 2017 and 2021 (see Table 1). The Shuttle Radar Topography Mission DEM (SRTM DEM) was used in this study. The road map was obtained from the Department of Environment and Natural Resources (DENR). The LULC maps were obtained from the ESRI land cover generated from Sentinel-2 10-m resolution (https://livingatlas.arcgis.com/landcover/). The elevation and distance to the road network were utilized as the exploratory data for LULC modeling (see Table 1 and Fig. 2). The land use classifications are shown in Table 2.

4. Methodology

Fig. 3 serves as a visual representation of the methodological framework utilized in this study, providing an overview of the processes and approaches employed. Within this figure, The 2017 and 2021 maps from ESRI (https://livingatlas.arcgis.com/landcover/) are featured, serving as valuable data sources for the analysis.

The final map (i.e., LULC, 2021) is produced using the ANN model from several images taken throughout the years. This approach allows for the integration of temporal information and can improve the land cover map's overall accuracy by capturing seasonal vegetation cover variations. In recent years, ANN modeling for land cover mapping has been demonstrated to be effective. Chen et al. (2020) used a machine-learning model trained on the Sentinel-2 dataset with an accuracy rate of 92.41%. This shows that the machine learning model effectively classifies and analyzes satellite imagery datasets.

The study used the ANN model to evaluate the impact of elevation

Table 3
The LULC transition matrix displays the alterations in the LULC classifications from 2017 to 2021. The rows represent the LULC information for 2017, while the columns represent the corresponding information for 2021. The matrix presents a visual representation of the changes in LULC for each classification.

Classification	1	2	3	4	5	6	7	8
Water (1)	0.861	0.075	0.003	0.031	0.019	0.004	0.0002	0.007
Trees (2)	0.001	0.923	0.00002	0.013	0.024	0.0004	0.001	0.037
Flood Vegetation 3	0.268	0.513	0.134	0.031	0.041	0	0.0007	0.012
Crops (4)	0.005	0.269	0.00001	0.587	0.097	0.0006	0.004	0.038
Built Area (5)	0.001	0.027	0.00003	0.007	0.962	0.0003	0.0006	0.002
Bare Ground (6)	0.022	0.140	0.0001	0.022	0.720	0.048	0.0008	0.048
Clouds (7)	0.0002	0.856	0	0.035	0.051	0.003	0.029	0.026
Rangeland (8)	0.0007	0.340	0.00009	0.042	0.029	0.002	0.003	0.583

Table 4
The changes in LULC classifications from 2017 to 2021 are depicted in this analysis, providing insight into the alterations in each classification (m^2).

Classification	2017	2021	Δ	2017%	2021%	Δ %
Water (1)	17155100	18195800	1040700	0.7718	0.818	0.0468
Trees (2)	1697089000	1698246400	1157400	76.280	76.332	0.0528
Flood Vegetation (3)	968400	243900	−724500	0.04358	0.011	−0.033
Crops (4)	118832900	101264600	−17568300	5.341	4.552	−0.790
Built Area (5)	183654100	240669200	57015100	8.255	10.817	2.563
Bare Ground (6)	5547100	1712100	−3835000	0.249	0.077	−0.172
Clouds (7)	45413400	4574600	−40838800	2.041	0.206	−1.836
Rangeland (8)	156162300	159915700	3753400	7.019	7.188	0.169

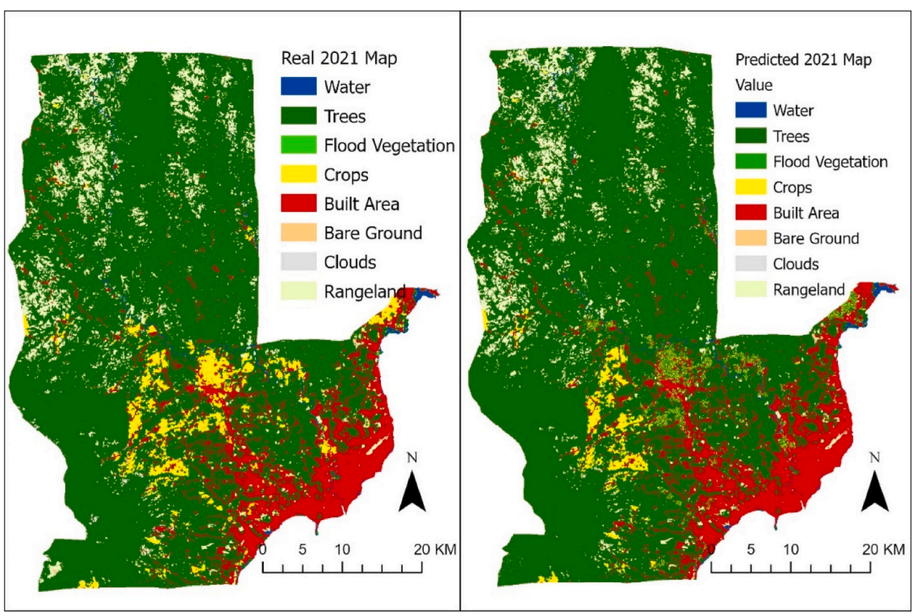

Fig. 4. LULC map comparison between (left) the baseline map and (right) the predicted map.

and distance to the road network on the LULC maps. This study used the elevation and distance of the road network datasets. These are raster datasets. The changes in each LULC category were determined by superimposing these rasters on top of the existing LULC maps. This process will detect the changes in the land. Then, a transition matrix was used to show the proportions of pixels that transitioned from one LULC category to another. A transition matrix is a tool in change detection studies. It allows identifying patterns and trends in land use change over time. The comparison of the two rasters helped examine the relationship between LULC. Thus, it provides valuable insights into the dynamic changes in LULC. This insight contributes to a better understanding of the factors influencing LULC dynamics and assists land management and planning.

The created map was evaluated to determine the quality of the LULC classification. The kappa coefficient (KC) and overall accuracy (OA) metrics were used to evaluate the LULC map. The OA is the percentage of correctly classified observations according to pixels in the classification. The OA also indicates how well the model predicts the true category across classes. The OA was computed using Equation (1).

$$OA = \frac{Sk}{S} x\ 100 \tag{1}$$

where k represents the area of interest, Sk is the number of correct samples, and S is the total sample.

Furthermore, the KC is frequently used to evaluate and assess the correctness of LULC maps. It was used to compare a simulated LULC map to a reference LULC map from 2021. The KC assesses the agreement between the two maps while accounting for the probability of chance agreement. The following Equation (2) was used in computing the KC index.

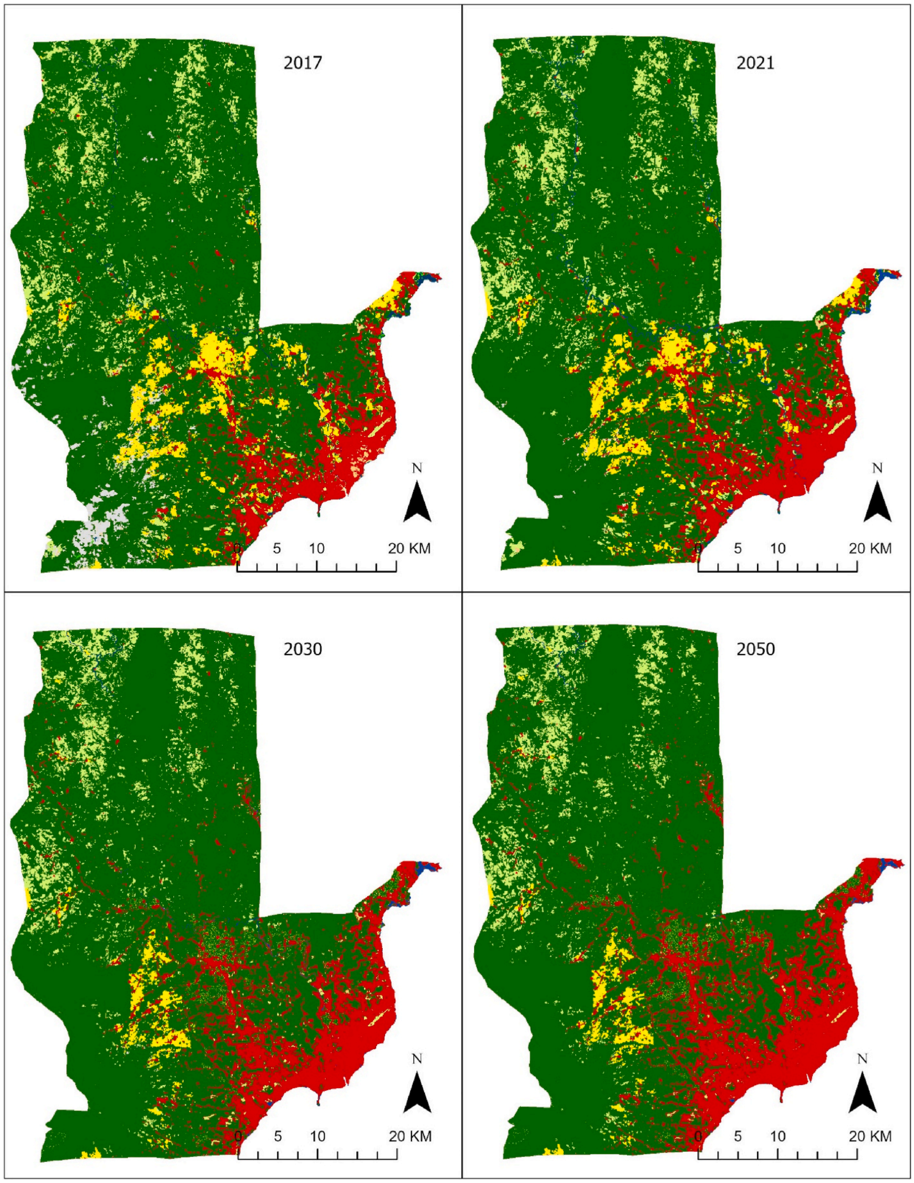

Fig. 5. LULC map comparison between the baseline map and the predicted map. Top-left and top-right are the 2017 baseline map and 2021 reference map for modeling, respectively. The predicted maps for 2030 and 2050 are displayed in the bottom left and bottom right, respectively.

Table 5
LULC change matrix between the predicted and baseline map in 2021. A positive and negative value indicates the increase and decrease in the classifications, respectively.

Classification	Predicted (2030) – Real (2017)		Predicted (2050) – Real (2017)	
	Δ m^2	Δ %	Δ m^2	Δ %
Water (1)	−7,534,800	−0.34	−11,821,300	−0.53
Trees (2)	51,319,900	2.31	13,818,200	0.62
Flood Vegetation (3)	−796,400	−0.04	−877,600	−0.04
Crops (4)	−72,412,600	−3.25	−73,883,200	−3.32
Built Area (5)	100,012,200	4.50	153,361,900	6.89
Bare Ground (6)	−4,451,700	−0.20	−4,809,400	−0.22
Clouds (7)	−44,714,200	−2.01	−44,888,400	−2.02
Rangeland (8)	−21,422,400	−0.96	−30,900,200	−1.39

$$KC = \frac{Po - Pe}{1 - Pe} \tag{2}$$

where Po is the proportion of observed agreements, and Pe is the proportion of agreements expected by chance (Saputra and Lee, 2019).

In this example, the KC is used to validate the simulated 2021 LULC map against the reference map of the real 2021 LULC map. KC allows evaluation of how well the ANN model predicted the area's current land cover. Furthermore, following the validation process, future LULC maps for 2030 and 2050 were estimated by assuming the continuation of the current land use change patterns. The weights utilized in simulating the 2021 LULC map were applied to the neural network in simulating future LULC changes. This can give current and future insights into the potential land use pattern and provide an understanding of land use planning and management decisions.

5. Results and discussion

5.1. Transition and prediction scenario

A transition matrix was used as an input in a neural network analysis to quantify the rate of change in LULC. The neural network created the final LULC output by calculating the likelihood of change in each input. The relative proportions of various LULC categories between 2017 and 2021 were compared to produce the LULC transition matrix, shown in Tables 3 and 4.

The transition matrix values show the changes from each classification to another classification. The transition modeling from 2017 to 2021 depicts that water, trees, built area, and rangeland increase over time. In contrast, the changes in the land have a detrimental impact on the flood vegetation, crops, bare ground, and clouds. The built area classification has the highest positive increase of the land with approximately 2.56% or 240.669 km^2, while the crop classification decreases around 0.79% or 101.265 km^2.

This information helps us understand the patterns and trends of LULC changes over time. By analyzing the LULC transition matrix, decision-makers can plan and implement effective, sustainable land use management and conservation strategies. Moreover, the insights generated from the neural network model can be leveraged for various purposes, such as urban planning, environmental management, and natural resource management.

In summary, this study aimed to utilize an ANN model to predict future LULC in 2021 by considering exploratory maps such as the distance from road networks and elevation. The accuracy of the predictions was evaluated by comparing the predicted LULC for 2021 with the 2021 LULC map obtained from ESRI. The results demonstrated a high level of accuracy, with a percentage of correctness of 96.68% and a Kappa score of 0.91. This shows that the projected and actual maps are very close, as presented in Fig. 4. The similarities between the two maps were almost indistinguishable. These findings highlight the effectiveness of the method in forecasting future LULC changes.

5.2. Projected scenario

The prediction maps show the projected land use scenario in 2030 and 2050 (see Fig. 5). Table 5 gives the square meters and percentages of the land changes based on the 2017 baseline map. The four maps are shown in Fig. 5.

The 2017 baseline map is in the top-left, while the 2019 LULC is in the top-right of the image. Moreover, the bottom-left and bottom-right are the predicted LULC for 2030 and 2050, respectively.

According to the projections, the built area and tree cover are expected to increase by approximately 4.50% and 2.31% by 2030. However, crops will drastically decrease by up to 3.25%, or approximately 464.203 km^2 will be lost. Furthermore, the water, flood vegetation, bare ground, clouds, and rangeland will decrease around 0.34% (753.48 km^2), 0.04% (796.40 km^2), 0.20% (445.17 km^2), 2.00% (447.14 km^2) and 0.96% (214.22400 km^2), respectively.

In 2050, the built area will continue to increase to 6.89% or approximately 337.02 km^2. In contrast, the trees will decrease from 2.31% in 2030 to 0.62% in 2050. This demonstrates how land changes are affected by human activities. This result also reflects that Davao City is driving toward heavy industrialization and urbanization in the future. The agricultural related classification like crops, flood vegetation, bare ground, and rangeland will be heavily affected in the future; around 738.83 km^2, 877.60 km^2, 480.94 km^2, and 309.00 km^2 will be lost, respectively. Water-related classifications (i.e., water, flood vegetation, and cloud coverage) are also affected. Table 5 shows the complete percentage change in these classifications. These findings have important implications for the city's future land use planning and resource management. As Davao City continues to grow and change, it is crucial to consider the long-term impact of these developments and implement sustainable practices to minimize harm to the natural environment and ensure a balanced relationship between human activities and the environment.

6. Conclusions

The LULC is essential as a basis for resource monitoring and planning activities. The LULC can assist in developing plans to balance development and conservation. This study applies the MLP-ANN model to predict changes in LULC in Davao City, Philippines.

The elevation and distance to the road network are derived from DEM and used as exploratory maps to train the MLP-ANN model. The exploratory maps for 2017 and 2021 show significant impacts on land changes in the simulation. The accuracy rate and Kappa index show that the predicted and actual maps for 2021 are in very high agreement. The MLP-ANN model was also employed to forecast how land will be used in 2030 and 2050.

The prediction models for 2030 and 2050 show a high increase in the built area, up to 6.89%, based on the 2017 baseline map. The trees classification will increase by approximately 2.31% in 2030, but it will slightly increase in the year 2050. Meanwhile, the crop area will decrease to around 464.203 km^2 (3.25%) and 738.83 km^2 (3.32%) in 2030 and 2050, respectively. This indicates that human activities influence the LULC change from agricultural land classifications to the built area.

The findings of this study provide valuable insights into the complex land use patterns of highly urbanized coastal cities like Davao City in the Philippines. Urbanization is the primary reason for the decline in crops and other agricultural and natural landscapes, emphasizing the importance of proper land use planning to balance development and environmental conservation where humans and the environment co-exist.

The use of the MLP-ANN model in this study provides a valuable tool for predicting future changes in the landscape. However, the results can be improved by including the impact of climate change and other meteorological and hydrological parameters. Addressing these limitations will broaden the understanding of how land use patterns evolve in Davao City and help inform future sustainable development strategies.

Author contributions

The conceptualization, analysis, and writing were conducted by both authors.

Declaration of competing interest

The authors declare that they have no known competing financial interests or personal relationships that could have appeared to influence the work reported in this paper.

Acknowledgments

The authors express gratitude to the University of Southeastern Philippines for the opportunity to conduct this research.

References

Amgoth, A., Rani, H.P., Jayakumar, K.V., 2023. Exploring LULC changes in Pakhal Lake area, Telangana, India using QGIS MOLUSCE plugin. Spatial Information Research. https://doi.org/10.1007/s41324-023-00509-1.

Bocco, M., Sayago, S., Willington, E., 2014. Neural network and crop residue index multiband models for estimating crop residue cover from Landsat TM and ETM+ images. Int. J. Rem. Sens. 35 (10), 3651–3663. https://doi.org/10.1080/01431161.2014.915436.

Cabrera, J.S., Lee, H.S., 2022. Coastal zone environment Integrity assessment for sustainable management: Part 1. Development of Adaptive Expert-Driven coastal zone Health index framework. J. Mar. Sci. Eng. 10 (Issue 9) https://doi.org/10.3390/jmse10091183.

Cengiz, A., Budak, M., YAĞMUR, N., BALÇIK, F., 2023. Comparison between random forest and support vector machine algorithms for LULC classification. International Journal of Engineering and Geosciences 8 (1), 1–10.

Chang, Y., Hou, K., Li, X., Zhang, Y., Chen, P., 2018. Review of land Use and land cover change research progress. IOP Conf. Ser. Earth Environ. Sci. 113 (1) https://doi.org/10.1088/1755-1315/113/1/012087.

Chao, Z., Zhao, Y., Liu, G., 2022. Multi-scale spatial patterns of Gelugpa monasteries of Tibetan Buddhism in Tibetan inhabited regions, China. Geojournal 87 (5), 4289–4310. https://doi.org/10.1007/s10708-021-10501-7.

Dinda, S., Chatterjee, N. Das, Ghosh, S., 2022. Modelling the future vulnerability of urban green space for priority-based management and green prosperity strategy planning in Kolkata, India: a PSR-based analysis using AHP-FCE and ANN-Markov model. Geocarto Int. 37 (22), 6551–6578. https://doi.org/10.1080/10106049.2021.1952315.

FAO, 2007. Land Use, Land-Use Change and Forestry: Special Report of the Intergovernmental Panel on Climate Change. Cambridge University Press.

Handayani, H.H., Murayama, Y., Ranagalage, M., Liu, F., Dissanayake, D.M.S.L.B., 2018. Geospatial analysis of horizontal and vertical urban expansion using multi-spatial resolution data: a case study of Surabaya, Indonesia. Rem. Sens. 10 (10) https://doi.org/10.3390/rs10101599.

Houghton, R.A., House, J.I., Pongratz, J., Van Der Werf, G.R., Defries, R.S., Hansen, M.C., Le Quéré, C., Ramankutty, N., 2012. Carbon emissions from land use and land-cover change. Biogeosciences 9 (12), 5125–5142.

Isabona, J., Imoize, A.L., Ojo, S., Karunwi, O., Kim, Y., Lee, C.-C., Li, C.-T., 2022. Development of a multilayer perceptron neural network for optimal predictive modeling in urban microcellular radio environments. Appl. Sci. 12 (11), 5713.

Jie, C., Jing-Zhang, C., Man-Zhi, T., Zi-tong, G., 2002. Soil degradation: a global problem endangering sustainable development. J. Geogr. Sci. 12, 243–252.

Kelly-Fair, M., Gopal, S., Koch, M., Pancasakti Kusumaningrum, H., Helmi, M., Khairunnisa, D., Kaufman, L., 2022. Analysis of land Use and land cover changes through the Lens of SDGs in Semarang, Indonesia. Sustainability 14 (13). https://doi.org/10.3390/su14137592.

Koh, L.P., Wilcove, D.S., 2008. Is oil palm agriculture really destroying tropical biodiversity? Conservation Letters 1 (2), 60–64. https://doi.org/10.1111/j.1755-263X.2008.00011.x.

Lambin, E.F., Geist, H.J., Lepers, E., 2003. Dynamics of land-use and land-cover change in tropical regions. Annu. Rev. Environ. Resour. 28 (1), 205–241. https://doi.org/10.1146/annurev.energy.28.050302.105459.

Losiri, C., Nagai, M., Ninsawat, S., Shrestha, R.P., 2016. Modeling urban expansion in Bangkok Metropolitan region using demographic–economic data through cellular Automata-Markov chain and multi-layer perceptron-Markov chain models. Sustainability 8 (7). https://doi.org/10.3390/su8070686.

Megahed, Y., Cabral, P., Silva, J., Caetano, M., 2015. Land cover mapping analysis and urban growth modelling using remote sensing techniques in Greater Cairo Region—Egypt. ISPRS Int. J. Geo-Inf. 4 (3), 1750–1769.

Pijanowski, B.C., Brown, D.G., Shellito, B.A., Manik, G.A., 2002. Using neural networks and GIS to forecast land use changes: a Land Transformation Model. Comput. Environ. Urban Syst. 26 (6), 553–575. https://doi.org/10.1016/S0198-9715(01)00015-1.

PSA, 2020. 2020 Census of Population and Housing (2020 CPH) Population and Annual Growth Rates by Province, City, and Municipality - by Region.

Ren, Y., Lü, Y., Comber, A., Fu, B., Harris, P., Wu, L., 2019. Spatially explicit simulation of land use/land cover changes: current coverage and future prospects. Earth Sci. Rev. 190 (December 2018), 398–415. https://doi.org/10.1016/j.earscirev.2019.01.001.

Saputra, M.H., Lee, H.S., 2019. Prediction of land use and land cover changes for North Sumatra, Indonesia, using an artificial-neural-network-based cellular automaton. Sustainability 11 (11), 1–16. https://doi.org/10.3390/su11113024.

Sato, S., Tojo, B., Hoshi, T., Izni, L., Minsong, F., Moji, K., Kita, K., 2019. Recent Incidence of human Malaria caused by Plasmodium knowlesi in the Villages in Kudat Peninsula , Sabah , Malaysia : mapping of the Infection Risk using remote sensing data. Int. J. Environ. Res. Publ. Health 16 (16), 1–10.

Seto, K.C., Fragkias, M., Güneralp, B., Reilly, M.K., 2011. A meta-analysis of global urban land expansion. PLoS One 6 (8), e23777.

Seto, K.C., Güneralp, B., Hutyra, L.R., Luo, M., Hu, G., Chen, G., Liu, X., Hou, H., Li, X., 2022. Global forecasts of urban expansion to 2030 and direct impacts on biodiversity and carbon pools. Proc. Natl. Acad. Sci. USA 109 (1), 110. https://doi.org/10.1038/s41597-022-01204-w.

Sharma, R., Rimal, B., Stork, N., Baral, H., Dhakal, M., 2018. Spatial assessment of the potential impact of infrastructure development on biodiversity conservation in Lowland Nepal. ISPRS Int. J. Geo-Inf. 7 (Issue 9) https://doi.org/10.3390/ijgi7090365.

Silva, L. P. e, Xavier, A.P.C., da Silva, R.M., Santos, C.A.G., 2020. Modeling land cover change based on an artificial neural network for a semiarid river basin in northeastern Brazil. Global Ecology and Conservation 21, e00811. https://doi.org/10.1016/j.gecco.2019.e00811.

Talukdar, S., Singha, P., Shahfahad, Mahato, S., Praveen, B., Rahman, A., 2020. Dynamics of ecosystem services (ESs) in response to land use land cover (LU/LC) changes in the lower Gangetic plain of India. Ecol. Indicat. 112, 106121 https://doi.org/10.1016/j.ecolind.2020.106121.

Tran, H.T., Campbell, J.B., Wynne, R.H., Shao, Y., Phan, S.V., 2019. Drought and human impacts on land use and land cover change in a Vietnamese coastal area. Rem. Sens. 11 (3), 1–23. https://doi.org/10.3390/rs11030333.

Vadrevu, K., Heinimann, A., Gutman, G., Justice, C., 2019. Remote sensing of land use/cover changes in South and Southeast Asian Countries. International Journal of Digital Earth 12 (10), 1099–1102. https://doi.org/10.1080/17538947.2019.1654274.

Verburg, P.H., Schot, P.P., Dijst, M.J., Veldkamp, A., 2004. Land use change modelling: current practice and research priorities. Geojournal 61 (4), 309–324. https://doi.org/10.1007/s10708-004-4946-y.

Vorosmarty, C.J., Green, P., Salisbury, J., Lammers, R.B., 2000. Global water resources: vulnerability from climate change and population growth. Science 289 (5477), 284–288.

Xia, T., Wu, W., Zhou, Q., Verburg, P.H., Yu, Q., Yang, P., Ye, L., 2016. Model-based analysis of spatio-temporal changes in land use in Northeast China. J. Geogr. Sci. 26 (2), 171–187. https://doi.org/10.1007/s11442-016-1261-8.

Xiao, Y., Zhong, J.-L., Zhang, Q.-F., Xiang, X., Huang, H., 2022. Exploring the coupling coordination and key factors between urbanization and land use efficiency in ecologically sensitive areas: a case study of the Loess Plateau, China. Sustain. Cities Soc. 86, 104148.

Zhu, Z., Zhang, Z., Zhao, X., Zuo, L., Wang, X., 2022. Characteristics of land Use change in China before and after 2000. Sustainability 14 (Issue 21). https://doi.org/10.3390/su142114623.